Neuron, Vol. 30, 411–422, May, 2001, Copyright ©2001 by Cell Press

Proprioceptor Pathway Development Is Dependent on MATH1

Nessan A. Bermingham,[1,2] Bassem A. Hassan,[2] Vincent Y. Wang,[3] Michael Fernandez,[1,2] Sandro Banfi,[5] Hugo J. Bellen,[1,2,3] Bernd Fritzsch,[6] and Huda Y. Zoghbi[1,2,3,4,7]

[1] Howard Hughes Medical Institute
[2] Department of Molecular and Human Genetics
[3] Program in Developmental Biology
[4] Department of Pediatrics
Baylor College of Medicine
One Baylor Plaza
Houston, Texas 77030
[5] Telethon Institute of Genetics and Medicine
Via Olgettina 58
20132 Milan
Italy
[6] Department of Biomedical Sciences
Creighton University
2500 California Plaza
Omaha, Nebraska 68178

Summary

The proprioceptive system provides continuous positional information on the limbs and body to the thalamus, cortex, pontine nucleus, and cerebellum. We showed previously that the basic helix-loop-helix transcription factor *Math1* is essential for the development of certain components of the proprioceptive pathway, including inner-ear hair cells, cerebellar granule neurons, and the pontine nuclei. Here, we demonstrate that *Math1* null embryos lack the D1 interneurons and that these interneurons give rise to a subset of proprioceptor interneurons and the spinocerebellar and cuneocerebellar tracts. We also identify three downstream genes of *Math1* (*Lh2A, Lh2B,* and *Barhl1*) and establish that *Math1* governs the development of multiple components of the proprioceptive pathway.

Introduction

The sensory system carries information from internal and external receptors to the central nervous system (CNS), where this information is processed to direct movement. The sensory pathways can be divided into exteroceptive and proprioceptive: the former mediates sensations of touch, temperature, and pain, while the latter mediates positional information (i.e., the position of body parts with respect to each other). The two pathways are interlinked and jointly modulate motor responses.

Initiation and control of movement requires proprioceptive input from various receptors located in the skin, inner ear, muscles, tendons, and joints. Control of movement is further refined by input from inhibitory interneurons that regulate motor pathways (Martin, 1996; Tracey, 1995). As depicted in Figure 1A, proprioceptive signals are transferred via sensory neurons, interneuronal tracts, and central nuclei. These include the dorsal root ganglia (DRG), spinocerebellar tracts (SCTs), vestibular nuclei, thalamus, sensory cortex, pontine nucleus, and cerebellar granule neurons.

Previous studies have identified a number of genes required for the formation of individual components of the proprioceptive pathway. The basic helix-loop-helix (bHLH) genes *Ngn1* and *Ngn2,* for example, are necessary for the development of sensory neurons in the DRG (Ma et al., 1999). Indeed, many members of the bHLH family have been implicated in neurogenesis (*Ngn*1, *Ngn*2, and *Mash1*) (Fode et al., 1998; Ma et al., 1998; Lo et al., 1997; Casarosa et al., 1999). Mice null for *Math1* (mouse atonal homolog 1, a bHLH protein) die at birth and lack the cerebellar granule cell layer, pontine nucleus, and inner-ear hair cells—all elements of the proprioceptive pathway (Ben-Arie et al., 1997; Ben-Arie et al., 2000; Bermingham et al., 1999). *Math1* is also expressed in the dorsal spinal cord, joint chondrocytes, Merkel cells of the skin, and gut epithelium (Akazawa et al., 1995; Ben-Arie et al., 1997; Ben-Arie et al., 2000).

The discovery of *Math1* expression in the developing spinal cord raised questions about its function in this structure and whether that function is relevant to the integrity of the proprioceptive pathway. The developing dorsal neural tube gives rise to neural crest cells (which, in turn, give rise to sensory neurons, among other cell types), roof plate cells, and associate (ipsilateral) and commissural (contralateral) interneurons (Lee and Jessell, 1999). In the mature spinal cord, axons from both ipsilateral and contralateral interneurons form ascending tracts projecting to the thalamus, brainstem, and cerebellum, carrying proprioceptive and exteroceptive information. Three populations of interneuronal precursors are specified in the dorsal spinal cord and can be distinguished by the expression of developmentally regulated transcription factors. As shown in Figure 1B, expression of *Lh2A*/*Lh2B* (Lim homeodomains 2A and 2B, respectively) defines the most dorsal group, the *Lh2A*-positive D1A and *Lh2B*-positive D1B interneuron precursors; *Islet1* (*Isl1*) expression defines the second group, the D2 interneuron precursors; and *lim1/2* expression defines the most ventral group of the dorsal spinal cord, the D3 interneuron precursors (Liem et al., 1997). It is unknown, however, which precursor population (D1, D2, or D3) contributes to which population of neurons in the spinal cord. Limited data—namely, coexpression of *Lh2* with commisural interneuron-specific markers TAG1 (transiently expressed glycoprotein 1) and DCC (deleted in colorectal cancer)—suggest that D1 cells give rise to some commissural interneurons (Dodd et al., 1988; Furley et al., 1990; Keino-Masu et al., 1996; Liem et al., 1997).

Helms and Johnson (1998) and Lee et al. (1998) demonstrated that MATH1 is coexpressed with LH2A/LH2B in D1 interneuron precursors. These interneuron precursors migrate in two waves: the first, involving the D1B cells, takes place between E10.5 and E12 to give rise

[7] Correspondence: hzoghbi@bcm.tmc.edu

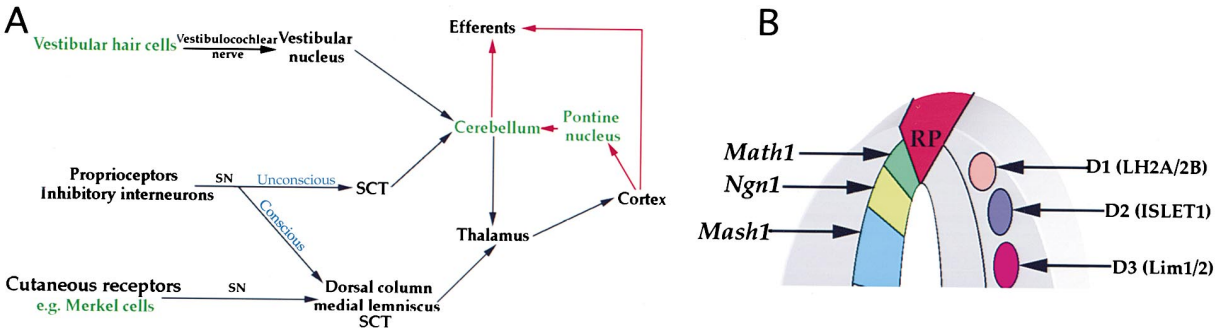

Figure 1. Afferent Proprioceptive Pathway and Dorsal Spinal Cord Neuronal Population

(A) Schematic outlining key components of the afferent proprioceptive pathway. Proprioceptive signals are transmitted from peripheral mechanoreceptors to the cerebellum and thalamus via the spinocerebellar tracts (SCT) or VIIIth cranial nerve prior to, during, and after movement. Unconscious proprioception is mediated through the cerebellum to the thalamus while conscious proprioception is mediated directly through the thalamus, bypassing the cerebellum. Information from the thalamus is transmitted to the cortex where it is processed and either relayed back to the cerebellum via the pontine nucleus for modulation or relayed directly to the efferent pathways. It should be noted that interactions occur between tracts and nuclei at each stage of the pathway. *Math1*-dependent components of the proprioceptive pathway are indicated in green; cortical output is indicated by red arrows. Spinocerebellar tract (SCT), sensory neurons (SN).

(B) Schematic of the dorsal spinal cord during development. Left side indicates the location of bHLH gene expression, while right shows location and interneuron precursors specific markers during development.

to certain neurons in the deep dorsal horn (Lee et al., 1998). The second wave, involving the D1A cells, takes place between E12 and E14 and gives rise to a population of neurons that also occupy the deep dorsal horn (Lee et al., 1998). In the absence of the bone morphogenetic protein GDF7, LH2A-positive D1 interneuron precursors fail to be specified after E12. The loss of LH2A expression coincides with a reduction in *Math1*-expressing cells and a dorsal shift in the *Ngn1* expression domain (Lee et al., 1998). Analysis of *Math1/lacZ* transgenic mice revealed that *lacZ* expression colocalizes with the pathfinding genes DCC and TAG1, further supporting the notion that *Math1* is involved in D1 interneuron precursor development (Helms and Johnson, 1998).

In this study, we demonstrate that in the absence of *Math1,* the precursors to the D1 interneurons fail to be specified and that the D1 interneuron precursors give rise to interneurons whose axons form the spinocerebellar tracts.

Results

Math1 Is Required for Ventral Migration of D1 Interneuron Precursors and for a Subpopulation of Commissural Interneurons

To gain insight into *Math1*'s role in the development of the dorsal spinal cord, we studied whole-mount and horizontal sections through the spinal cord for *lacZ* expression in the knock-in *Math1*$^{\beta\text{-Gal}/+}$ and *Math1*$^{\beta\text{-Gal}/\beta\text{-Gal}}$ embryos from E9.5 to E14.5. (Throughout this report, we use the term "*lacZ* expression" to signify the X-gal reaction product.) In the *Math1*$^{\beta\text{-Gal}}$ knock-in allele, the *Math1* coding region is replaced by the coding region of β-galactosidase. Thus *Math1*$^{\beta\text{-Gal}/\beta\text{-Gal}}$ mice are null for MATH1 (Ben-Arie et al., 2000). We first detected *Math1/lacZ* expression in *Math1*$^{\beta\text{-Gal}/+}$ embryos at E9.5 adjacent to neural tube cells that give rise to neural crest and roof plate cells (Ben-Arie et al., 2000). Expression bilateral to the roof plate is apparent by E10.5, with ventrally projecting *lacZ*-positive fibers emanating from the dorsal spinal cord (Figure 2A). At E11.5, staining remains bilateral, but *lacZ*-positive cells are observed ventrally, appearing to accumulate in the deep dorsal horn and projecting fibers across the floor plate (Figure 2C). *LacZ*-positive axons crossing the floor plate were observed in 45 μm sections of *Math1*$^{\beta\text{-Gal}/+}$ embryos; this indicates that at least some of the cells are commissural interneurons (Altman and Bayer, 1984) (Figure 2E). *LacZ* expression in the dorsal part of spinal cord begins to decline at E12.5 (arrow, Figure 2G), whereas expression in the ventral domain is stronger than dorsal expression at that stage (arrowhead, Figure 2G). Although *lacZ*/β-gal expression projects ventrally and accumulates in the deep dorsal horn (Figures 2G and 2I), *Math1*'s RNA expression flanks the roof plate at that age (Figure 2I, inset). These observations indicate that cells arising from the *Math1*-positive domain first express lower levels of *Math1* and then migrate ventrally between E9.5 and E12.5. The stability of the β-gal protein allows *Math1/lacZ* expression to remain detectable in these cells during their migration to the deep dorsal horn. By E13.5 *lacZ* expression in the dorsal spinal cord is downregulated in a rostral/caudal manner, which is reminiscent of the spatial development of the spinal cord.

LacZ expression in *Math1*$^{\beta\text{-Gal}/\beta\text{-Gal}}$ embryos is significantly different from that observed in *Math1*$^{\beta\text{-Gal}/+}$ embryos. Expression begins at E9.5, but by E10.5 it appears to be dorsal with no apparent ventral projections (Figure 2B). By E11.5, some ventral *lacZ* projections are visible, but dorsal *lacZ* expression flanking the roof plate predominates (Figure 2D). Significantly fewer *lacZ*-positive axons cross the floor plate in *Math1*$^{\beta\text{-Gal}/\beta\text{-Gal}}$ embryos than in heterozygous animals (Figure 2F). At E12.5, most of the *lacZ*-stained cells remain at the dorsal aspect of the spinal cord in the *Math1*$^{\beta\text{-Gal}/\beta\text{-Gal}}$ animals, in contrast to the few *lacZ*-stained cells observed in the *Math1*$^{\beta\text{-Gal}/+}$ animals (Figures 2G–2J). Similarly, intense β-gal immunoreactivity adjacent to the roof plate in *Math1*$^{\beta\text{-Gal}/\beta\text{-Gal}}$

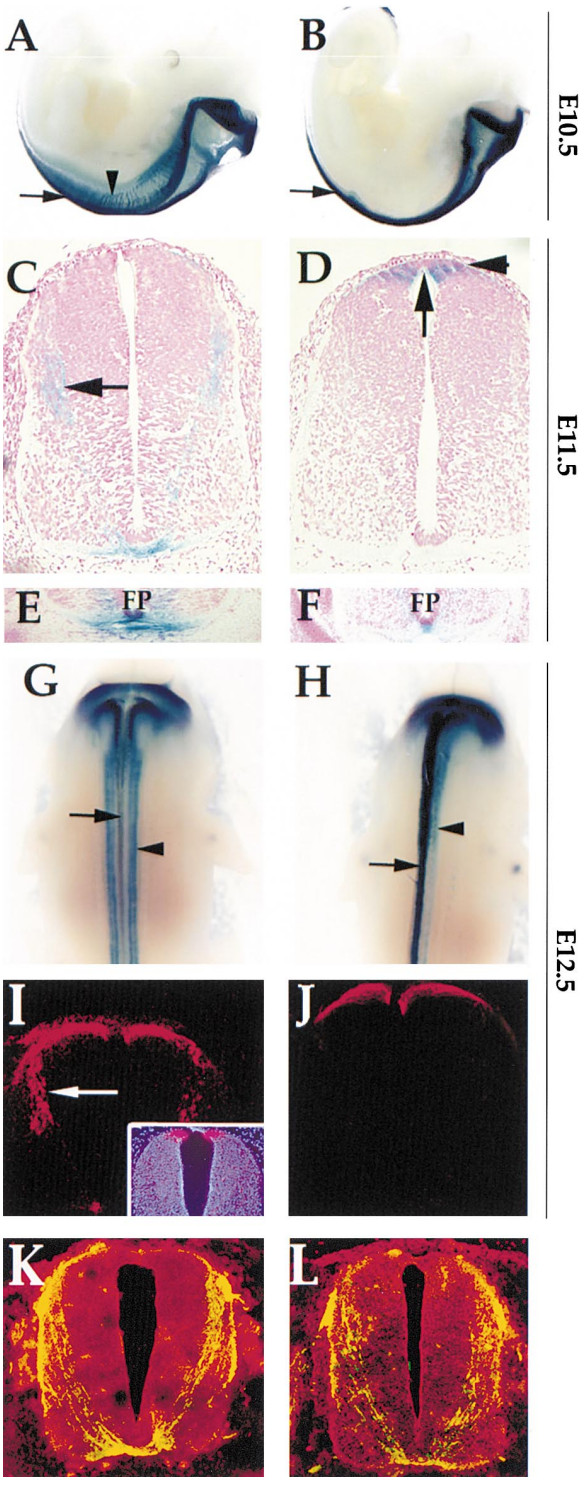

Figure 2. *Math1* Is Necessary for Mediolateral Migration of D1 Interneurons

(A and B) Whole-mount *lacZ* staining of E10.5 *Math1*$^{\beta\text{-Gal}/+}$ (A) and *Math1*$^{\beta\text{-Gal}/\beta\text{-Gal}}$ (B) embryos. Dorsal expression is observed in both heterozygote and null embryos (arrow), but ventral projections (A, arrowhead) are absent in nulls.

(C and D) Six μm cross sections through the spinal cord of E11.5 *Math1*$^{\beta\text{-Gal}/+}$ (C) and *Math1*$^{\beta\text{-Gal}/\beta\text{-Gal}}$ (D) *lacZ* stained embryos. *LacZ*-positive cells appear to accumulate in the deep dorsal horn in heterozygotes (arrow) while *lacZ*-positive cells flank (arrowhead) and begin to populate the roof plate (arrow) in *Math1* null embryos; no expression is observed in the deep dorsal horn.

(E and F) *LacZ*-positive fibers crossing the floor plate of heterozygote and, to a limited extent, null embryos are seen in 40 μm cross sections through the floor plate of E11.5 *Math1*$^{\beta\text{-Gal}/+}$ (E) and *Math1*$^{\beta\text{-Gal}/\beta\text{-Gal}}$ (F) embryos.

(G and H) Whole-mount *lacZ* expression of E12.5 *Math1*$^{\beta\text{-Gal}/+}$ (G) and *Math1*$^{\beta\text{-Gal}/\beta\text{-Gal}}$ (H) embryos. Dorsal expression is still evident (arrow) and some ventral projections are apparent in *Math1* null embryos (arrowhead).

(I and J) Immunofluorescence on cross sections through the spinal cord of E12.5 *Math1*$^{\beta\text{-Gal}/+}$ (I) and *Math1*$^{\beta\text{-Gal}/\beta\text{-Gal}}$ (J) embryos using anti-β-gal antibody. β-gal positive cells migrate from the dorsal spinal cord to accumulate in the deep dorsal horn in heterozygotes (arrow), whereas in *Math1* null embryos, β-gal positive cells flank the roof plate and fail to migrate. No ventral expression is observed in null embryos. Inset shows in situ hybridization of E12.5 wild-type embryo with *Math1* riboprobe.

(K and L) Immunofluorescence with anti-TAG1 (E11.5) on *Math1*$^{\beta\text{-Gal}/+}$ (K) and *Math1*$^{\beta\text{-Gal}/\beta\text{-Gal}}$ (L) embryos.

Original magnifications: (C) and (D) ×160, (E) and (F) ×400, and (I) and (L) ×100; scale bar, 100 μm; inset ×120.

embryos was apparent at E12.5 (Figure 2J). We observed no *lacZ*-positive cells in the deep dorsal horn of the spinal cord of the *Math1*$^{\beta\text{-Gal}/\beta\text{-Gal}}$ animals, although a few ventrally projecting *lacZ*-positive axons are detected (Figures 2F and 2H).

Because there are ventrally projecting *lacZ*-positive axons in both *Math1*$^{\beta\text{-Gal}/+}$ and *Math1*$^{\beta\text{-Gal}/\beta\text{-Gal}}$ embryos at E11.5 and E12.5, and expression of a *Math1/lacZ* transgene colocalizes with the commissural interneuron-specific markers DCC and TAG1 (Helms and Johnson, 1998), we analyzed the expression of these markers at E11.5 and E12.5. We found no obvious differences in either DCC or TAG1 expression between wild-type and *Math1*$^{\beta\text{-Gal}/\beta\text{-Gal}}$ embryos (Figure 2K and 2L, and data not shown). Because of the marked reduction in *lacZ*-positive commissural interneurons in *Math1*$^{\beta\text{-Gal}/\beta\text{-Gal}}$ embryos, however, we cannot exclude the possibility that a subpopulation of these cells may be absent.

Loss of Expression of *Lh2A, Lh2B,* and *Barhl1* in the Dorsal Spinal Cord of *Math1* Null Embryos

To determine whether loss of *Math1* affects D1A or D1B cells, we studied LH2A (also known as LHX2 or LH2 [Porter et al., 1997; Xu et al., 1993]) and LH2B (also known as LHX9 [Bertuzzi et al., 1996; Retaux et al., 1999]) expression in the D1 population of the dorsal spinal cord. Immunohistochemical studies at E10.5, E11.5, E12.5, and E13.5, using an antibody recognizing both LH2A and LH2B wild-type spinal cord, revealed a staining pattern reminiscent of *lacZ* expression. Cells initially express LH2A and LH2B in the *Math1* domain before migrating ventrally to occupy the deep dorsal horn (Figure 3A and data not shown) (Lee et al., 1998). In contrast, E10.5, E11.5, E12.5, and E13.5 *Math1*$^{\beta\text{-Gal}/\beta\text{-Gal}}$ embryos failed to exhibit LH2A- and LH2B-positive cells in the dorsal spinal cord (Figure 3B and data not shown). Further analysis of *Lh2A* and *Lh2B* expression by in situ hybridization showed no expression in the spinal cord of *Math1* null embryos (Figures 3C and 3D, and data not shown). Expression of *Lh2A* in cortical neurons is unaffected in *Math1*$^{\beta\text{-Gal}/\beta\text{-Gal}}$ embryos (Figures 3C and 3D, inset).

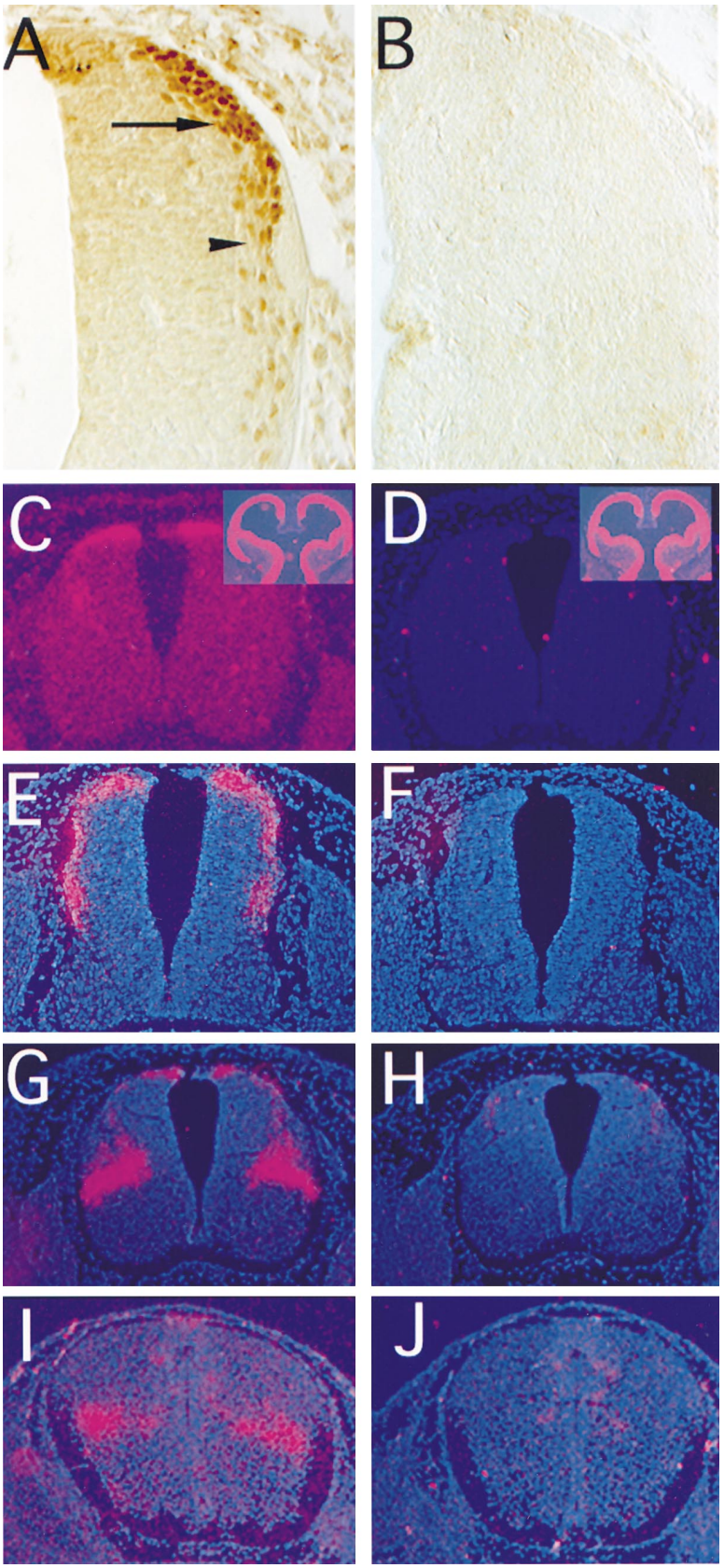

Figure 3. D1 Cells Fail to Express LH2A, LH2B, and *Barhl1* in the Spinal Cord of *Math1* Null Embryos

(A and B) Immunohistochemistry with anti-LH2A/LH2B antibody on spinal cord cross sections of E11.5 wild-type (A) and *Math1*$^{\beta\text{-Gal}/\beta\text{-Gal}}$ (B) embryos (half sections shown). LH2A and LH2B are expressed dorsally (arrow) and in ventrally migrating cells (arrowhead) in wild-type embryos, but no expression is observed in *Math1* null embryos.

(C and D) In situ hybridization with *Lh2A*-specific riboprobe on E11.5 spinal cord of wild-type (C) and *Math1*$^{\beta\text{-Gal}/\beta\text{-Gal}}$ (D) embryos. No expression is observed in the spinal cord of null embryos. Inset shows *Lh2A* expression in the cortex (where *Math1* is not expressed) of wild-type and null embryos.

(E–J) In situ hybridization with *Barhl1* specific riboprobe on E10.5 (E and F), E12.5 (G and H) and E13.5 (I and J), wild-type (E, G, and I) and *Math1*$^{\beta\text{-Gal}/\beta\text{-Gal}}$ (F, H, and J) embryos. Dorsal expression is evident with cells migrating ventrally, accumulating in the deep dorsal horn (arrowhead) in E13.5 wild-type embryos. No expression is observed in *Math1* null embryos at any stage examined.

Original magnifications: (A) and (B) ×200, (C) and (D) ×100, (E) and (F) ×160, and (G) and (J) ×120.

Given the absence of the LH2A and LH2B expression in the D1 interneuron precursors, we sought to determine whether other D1-specific genes such as *Barhl1* are also affected. A member of the Bar family of transcription factors, BarH-like 1 (*Barhl1*), was recently shown to be expressed in similar domains as *Math1*, including inner-ear sensory epithelia, the EGL of the cerebellum, the pontine nucleus, and the dorsal spinal cord (Bulfone et al., 2000). *Barhl1* is expressed in the dorsal aspect of the spinal cord in a pattern similar to that of *Math1/lacZ* and LH2A/ LH2B (Figures 3E, 3G, and 3I). *Barhl1*-positive cells migrate ventrally, coming to rest in the deep dorsal horn of the spinal cord between E10.5 and E13.5 (Figures 3E, 3G, and 3I). Analysis of *Math1*$^{\beta\text{-Gal}/\beta\text{-Gal}}$ embryos from E10.5 to E13.5 revealed a complete loss of *Barhl1* expression in the dorsal spinal cord and deep dorsal horn (Figures 3F, 3H, and 3J).

In summary, the loss of LH2A, LH2B, and *Barhl1* expression, and the loss of *lacZ* staining in the deep dorsal horn indicate that the D1 precursors are absent in the dorsal spinal cord of *Math1* null embryos.

Neural Crest Differentiation and Sensory Neuron Formation in the Absence of *Math1*

Neural crest cells derive from the dorsal region of spinal cord. Because *Math1* is expressed in the dorsal aspect of the spinal cord, we investigated whether neural crest formation is affected in *Math1*$^{\beta\text{-Gal}/\beta\text{-Gal}}$ animals. We generated mice carrying the neural crest reporter gene *Wnt-1-lacZ* on either a wild-type or null *Math1* background (Echelard et al., 1994). There was no obvious difference in reporter gene activity between the two lines of mice (data not shown). Neural crest derivatives, including melanocytes and various types of sensory neurons, also appear similar. Melanocytes of the inner ear appeared to be normal in *Math1* null embryos (data not shown). Whole-mount immunostaining as well as staining of sections with the neurofilament marker 2H3 showed no obvious defects in the cranial nerves or sensory neurons in *Math1* null embryos (data not shown, and Figures 4A and 4 B). Lastly, we performed in situ hybridization analysis of *trkA* (Figures 4C and 4D) and *trkC* (Figures 4E and 4F) in both wild-type and *Math1* null embryos. *trkA* is expressed in small-diameter nociceptive neurons (Ma et al., 1998; Martin, 1996), whereas *trkC* is expressed in large-diameter neurons mediating mechanoreception and proprioception (Ma et al., 1999; Martin, 1996). The lack of any appreciable difference between wild-type and *Math1* null embryos in expression of these two markers suggests that DRG differentiation is grossly normal in *Math1* mutants. Further analysis (e.g., cell counts, higher resolution tracing of axonal projections, etc.) is required to determine whether there are more subtle specification or differentiation effects.

Fate of *Math1*-Expressing Cells

What is the fate of *Math1*-expressing cells in *Math1*$^{\beta\text{-Gal}/\beta\text{-Gal}}$ embryos in the absence of *Math1*? We considered three possibilities: (1) the cells undergo apoptosis; (2) the cells undergo a fate switch; or (3) the cells remain undifferentiated.

To address these possibilities, we evaluated the spinal cords of wild-type and *Math1* null embryos at various stages for apoptosis, BrdU incorporation, expression of a mitotic marker, and expression of developmentally regulated genes.

Analysis of cell proliferation using BrdU incorporation and the mitotic marker anti-phosphohistone H3 antibody revealed no obvious differences between wild-type and *Math1* nulls from E11.5 to E13.5, nor did analysis of cell death using TUNEL reveal any differences in apoptosis. These results suggest that loss of *Math1* has no detectable effect on cellular proliferation or cell death between E11.5 and E13.5 (data not shown).

Math1-expressing cells (the D1A/D1B interneuron precursors) are known to reside between the ventral marker *Ngn1* and the dorsal roof plate markers *Gdf7* and *Msx-1* (Lee et al., 1998). To address the possibility of a fate switch, we performed in situ hybridization on spinal cord tissue from E11.5 and E12.5 embryos with *Gdf7* and *Ngn1* probes on alternate sections to determine whether their domains of expression were altered, as was observed for *Ngn1* in *Gdf7* null mice (Lee et al., 1998). RNA in situ analysis of *Ngn1* expression revealed no obvious difference between wild-type and *Math1* null embryos (Figures 5A and 5B). Similarly, *Gdf7* expression was not altered in *Math1* nulls (data not shown). These data indicate that neither the *Ngn1* nor *Gdf7* domains shifted or expanded in the absence of *Math1* (data not shown).

To further address the possibility of a fate switch in the absence of *Math1,* double-labeling immunofluorescence confocal analysis was carried out using an anti-β-galactosidase antibody and an antibody for either MSX1/2 (labeling the roof plate) or ISLET1 (labeling the D2 population of interneuron precursors) (Liem et al., 1995). MSX1/2 colocalized with a few medially located cells in *Math1*$^{\beta\text{-Gal}/+}$ embryos at the D1/roof plate junction (Figures 5C and 5E), whereas MSX1/2 colocalized with β-gal positive cells well beyond the D1/roof plate boundary in *Math1*$^{\beta\text{-Gal}/\beta\text{-Gal}}$ embryos (Figures 5D and 5F). This suggests that a subpopulation of β-gal-positive cells acquire roof plate properties in *Math1* null embryos. ISLET1 staining showed no colocalization with β-Gal in either *Math1*$^{\beta\text{-Gal}/+}$ (Figure 5G) or *Math1*$^{\beta\text{-Gal}/\beta\text{-Gal}}$ embryos (Figure 5H). These data, together with the lack of change in *Ngn1* or *Gdf7* expression, indicate that D1 interneuron precursors do not become D2 interneuron precursors in the absence of *Math1*.

Previous studies on dissociated dorsal spinal cord cells indicated that, in the absence of overlying epidermal ectoderm and roof plate cells (and, therefore, BMP signaling), cells entered a "default" pathway expressing the POU domain transcription factor BRN3A (Turner et al., 1997). Given the role of BMP in regulating the expression of *Math1* (Lee et al., 1998; Lee et al., 2000), we studied the expression of BRN3A in *Math1* null embryos. Immunofluorescence studies revealed a similar BRN3A-expression pattern in the dorsal spinal cord of *Math1*$^{\beta\text{-Gal}/+}$ (Figure 5I) and *Math1*$^{\beta\text{-Gal}/\beta\text{-Gal}}$ (Figure 5J) embryos. There was, however, a subpopulation of ventromedial BRN3A-positive cells detected in *Math1*$^{\beta\text{-Gal}/+}$ animals but missing in null mutants (Figure 5I, arrrowhead, and Figure 5J). This suggests that *Math1* is required for the formation of a subpopulation of BRN3A-positive cells that migrate ventromedially.

Lastly, we stained E18.5 spinal cords with either Nissl,

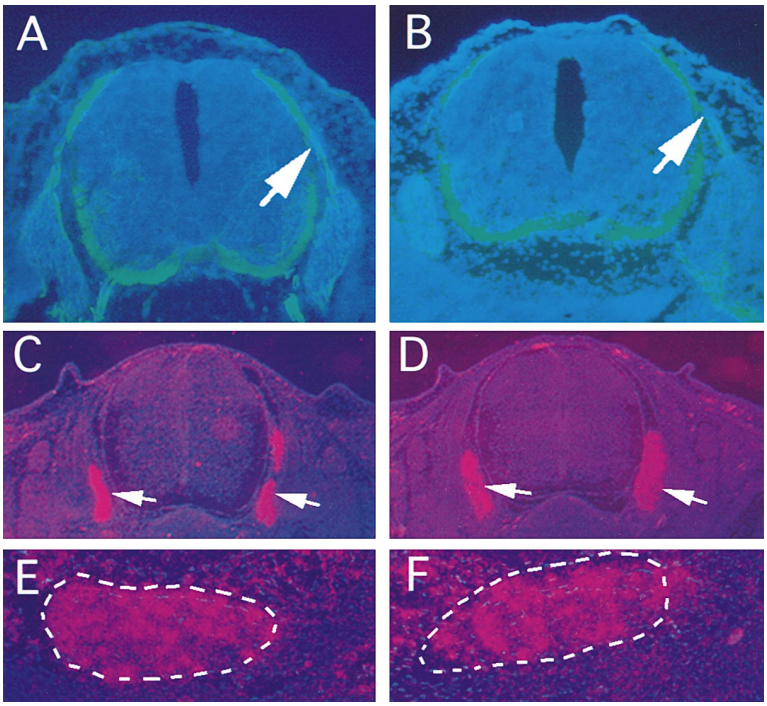

Figure 4. Analysis of Neural Crest Markers in *Math1* Null Animals

(A and B) Immunofluorescence with anti-2H3 antibody on E11.5 wild-type (A) and *Math1*$^{\beta\text{-Gal}/\beta\text{-Gal}}$ (B) embryos. Arrows indicate axons of the neural crest derived sensory neurons.

(C and D) In situ hybridization on E13.5 wild-type (C) and *Math1*$^{\beta\text{-Gal}/\beta\text{-Gal}}$ (D) embryos with *trkA*-specific riboprobe. Arrows indicate positively staining dorsal root ganglia.

(E and F) In situ hybridization on E13.5 wild-type (E) and *Math1*$^{\beta\text{-Gal}/\beta\text{-Gal}}$ (F) embryos with *trkC*-specific riboprobe. The dorsal root ganglia are outlined.

Original magnifications: (A) and (B) ×120, (C) and (D) ×100, and (E) and (F) ×160.

silverstain, or glial fibrillay acidic protein (GFAP). We observed no obvious abnormalities (data not shown). In summary, in the absence of *Math1* a subpopulation of the D1 precursor cells acquire roof properties as defined by MSX1/2 expression. Although BRN3A expression is retained dorsally, no expression is detected in the ventromedial region.

Math1-Dependent Interneurons Give Rise to a Subpopulation of the Dorsal and Ventral Spinocerebellar Tracts

Axons of neurons within the deep dorsal horn of the spinal cord project to the brain through a number of tracts, including the dorsal and ventral spinocerebellar tracts (SCTs). Four SCTs contain projections to the cerebellum and thalamus: the ipsilateral dorsal spinocerebellar tract (dSCT, originating from Clarke's column neurons), the ipsilateral cuneocerebellar (cSCT) tracts, the contralateral ventral (vSCT, which crosses again in the cerebellum), and ipsilateral rostral (rSCT) tracts (Tracey, 1995). The dSCT and vSCT are located in the spinal cord within laminae VI to VIII, encompassing the *Math1/lacZ*-expression domain. Both mediate proprioceptive and limited exteroceptive information from the lower limbs and lower trunk, whereas the cSCT (located in the medulla) and rSCT mediate information from the upper limbs and upper trunk (Tracey, 1995). The SCTs terminate within the thalamus or the spinocerebellar region of the cerebellum (Brodal, 1981; Brodal, 1998; Tracey, 1995).

To study those cells derived from the D1 population of interneuron precursors, we evaluated the integrity of the spinocerebellar and cuneocerebellar tracts in wild-type, heterozygote, and *Math1* null mice by DiI injection into both the target (cerebellum) and the origin of these fibers (spinal cord). Wild-type and *Math1*$^{+/\beta\text{-Gal}}$ mice showed massive bundles of crossed and uncrossed fibers at many levels of the brainstem, including fibers of the vSCTand dSCT; the external cuneate nucleus was also labeled by DiI (Figures 6A, 6C, and 6E). Contralateral neurons, such as the inferior olive and fastigial nuclei, were also labeled (Figure 6A). *Math1*$^{\beta\text{-Gal}/\beta\text{-Gal}}$ embryos, however, showed a reduction in the dSCT and vSCT, and the external cuneate nucleus was greatly reduced in size (Figure 6B). Injection of DiI into the external cuneate area labeled fibers running from the inferior cerebellar peduncle to the cerebellum revealed a diminished spinocerebellar and cuneocerebellar system, with very few fibers projecting into the cerebellum (data not shown). Other tracts labeled included the olivocerebellar, reticulocerebellar, and pontocerebellar fibers and vestibular projections. *Math1*$^{\beta\text{-Gal}/\beta\text{-Gal}}$ embryos showed a large reduction in the number of olivocerebellar and pontocerebellar tracts, but no differences were observed between *Math1*$^{\beta\text{-Gal}/\beta\text{-Gal}}$, wild-type, and *Math1*$^{+/\beta\text{-Gal}}$ embryos in the recticulocerebellar and vestibular neurons (Figures 6A–6F).

To determine whether *Math1/lacZ*-expressing neurons give rise to the spinocerebellar tracts, we carried out both DiI and *lacZ* labeling in cerebella and spinal cords of *Math1*$^{+/\beta\text{-Gal}}$ neonates according to a previously published protocol (Karis et al., 2001). *LacZ* colocalized with DiI in several areas studied, e.g., in the external cuneate nucleus (Figure 6G) and Clarke's nucleus (data not shown). Both populations provide ipsilateral cerebellar projections bringing proprioceptive information from the limbs to the cerebellum. We conclude that D1 interneuron precursors give rise to fibers of the dSCT and vSCT.

Discussion

Previous studies have demonstrated the essential role of *Math1* in the formation of the cerebellar granule neurons,

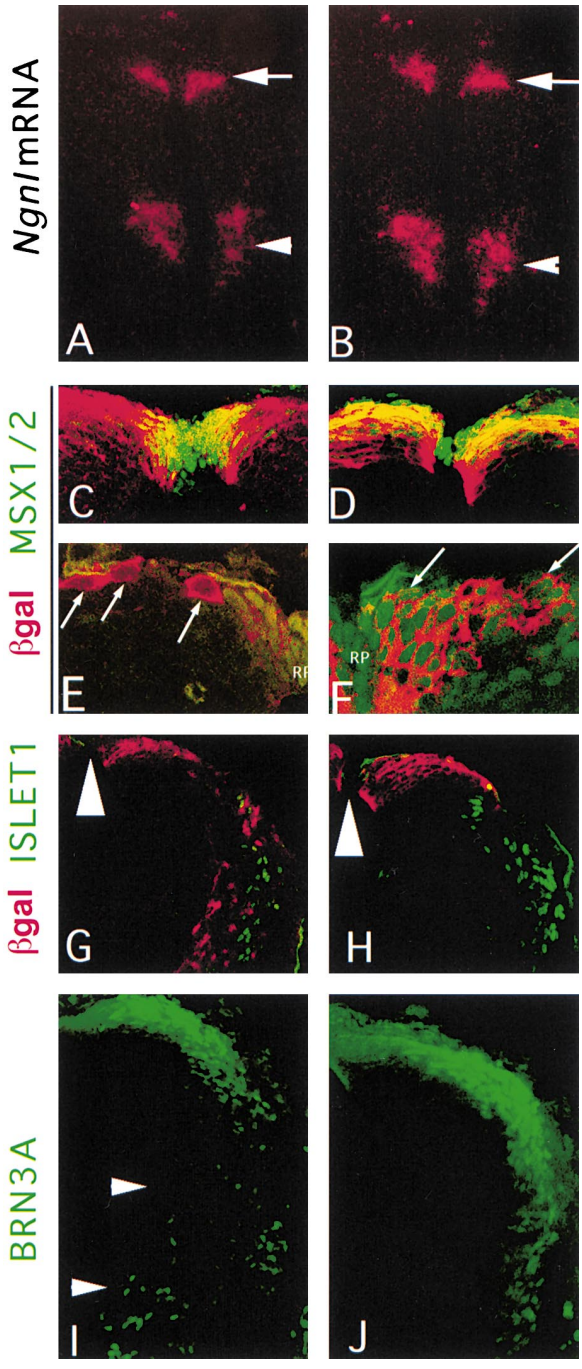

Figure 5. Cell Fate of D1 Precursors in the *Math1* Null Animals

(A and B) In situ hybridization with *Ngn1* specific riboprobe on E12.5 spinal cord of wild-type (A) and *Math1*$^{\beta\text{-Gal}/\beta\text{-Gal}}$ (B) embryos. Arrow indicates dorsal expression while arrowhead indicates *Ngn1* ventral expression.

(C and D) β-gal (red) and MSX1/2 (green) double-label immunofluorescence of *Math1*$^{\beta\text{-Gal}/+}$ (C) and *Math1*$^{\beta\text{-Gal}/\beta\text{-Gal}}$ (D) E12.5 embryos. MSX1/2 expression is evident in the roof plate and occasionally overlaps with β-gal at the D1/roof plate boundary in heterozygous embryos. *Math1* null embryos show an increase in the number of double-labeled cells lateral to the D1/roof plate boundary.

(E and F) Higher magnification of β-gal (red) and MSX 1/2 (green) double-label immunofluorescence of *Math1*$^{\beta\text{-Gal}/+}$ (E) and *Math1*$^{\beta\text{-Gal}/\beta\text{-Gal}}$ (F) E12.5 embryos. MSX 1/2 is expressed in the roof plate (RP) of the spinal cord. In the heterozygote animal, β-gal-expressing cells (red cytoplasmic staining in E) do not express MSX1/2; in contrast, most of the β-gal-expressing cells outside of the roof plate also express MSX1/2 (green nuclei in F) in the null mutant (arrow).

(G and H) β-gal (red) and ISLET1 (green) double-label immunofluorescence of *Math1*$^{\beta\text{-Gal}/+}$ (G) and *Math1*$^{\beta\text{-Gal}/\beta\text{-Gal}}$ (H) E12.5 embryos. ISLET1 expression is observed in the D2 population of interneurons and does not colocalize with β-gal expression in heterozygote or *Math1* null embryos.

(I and J) BRN3A immunofluorescence of *Math1*$^{\beta\text{-Gal}/+}$ (I) and *Math1*$^{\beta\text{-Gal}/\beta\text{-Gal}}$ (J) E12.5 embryos. BRN3A is expressed in the D1 domain. BRN3A-positive cells located in the medial aspect of the deep dorsal horn (I, arrows), appear to be absent in null embryos.

Original magnifications: (A) and (B) ×160, (C) and (D) ×400, (E) and (F) ×630, (G) and (H) ×250, and (I) and (J) ×160.

pontine nuclei, and inner-ear hair cells. Because the cerebellar granule neurons, pontine nuclei, and inner-ear hair cells are all involved in proprioception, we sought to determine whether *Math1* specifies other components of the proprioceptive system.

Math1 Specifies the D1 Population of Dorsal Interneurons

Lee et al. (1998) demonstrated that MATH1 is expressed within the D1 population of interneuron precursors that are dorsally defined before they migrate ventrally to the deep dorsal horn. *Math1*$^{\beta\text{-Gal}/+}$ embryos show *lacZ*-positive cells migrating to the deep dorsal region of the spinal cord, sending axonal projections across the floor plate, reminiscent of commissural interneurons. Null embryos show a different pattern of *lacZ* expression: *lacZ*-positive cells appear to accumulate at the dorsal spinal cord and fail to migrate ventrally. The presence of a few *lacZ*-positive axons that project ventrally and cross the floor plate, however, suggests that some *lacZ*-positive cells retain commissural interneuron properties.

Two closely related genes of the LH2 family, *Lh2A* and *Lh2B*, are expressed in the D1 population of interneuron precursors and mark distinct populations of cells: the D1A and D1B interneuron precursors, respectively (Lee et al., 1998). The absence of LH2A and LH2B expression in *Math1* nulls suggests a loss of D1 interneuron precursors. This is consistent with previous data from *Gdf7* mutants, in which *Math1* expression was reduced after E12, in conjunction with the downregulation of *Lh2A* expression and the loss of the D1A interneurons precursors (Lee et al., 1998).

LH2A and LH2B are members of the LIM homeodomain family of proteins believed to play important roles during development (Matsumoto et al., 1996; Xu et al., 1993). The expression pattern of *Lh2* genes and the ventral migration of *Lh2*-positive cells from the dorsal spinal cord lead us to believe that *Math1* may induce expression of the *Lh2* genes, which in turn may result in cell lineage differentiation of the D1 population of precursor cells. In the absence of *Math1,* LH2A and LH2B are not expressed, and the D1 precursors neither migrate nor differentiate. It is interesting to note that analysis of the 5′ upstream sequences of *Lh2A* (GenBank accession NM_010710) and *Lh2B* (GenBank accession NM_010714) indicates the presence of possible E-box sequences (CANNTG) at positions −58 to −53 (*Lh2A*, CACCTG) and −71 to −66 (*Lh2B*, CAGCTG). *Math1* associated with E47 has been previously shown to bind CAGCTG, initiating transcription of a down-

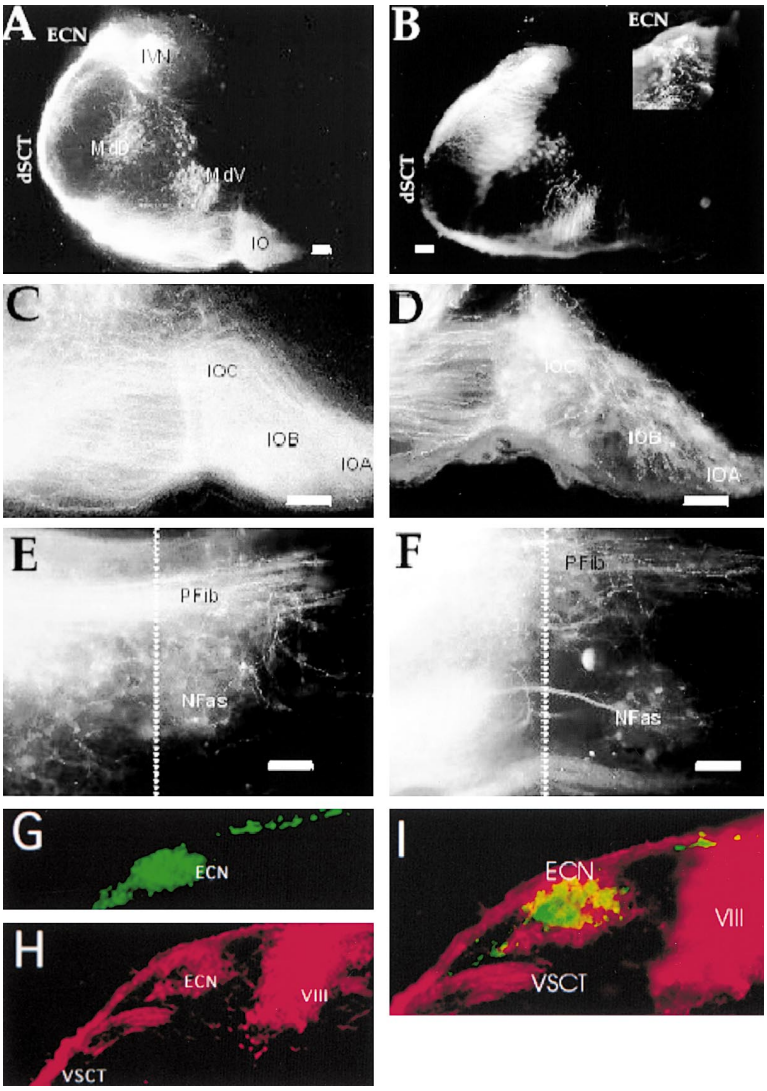

Figure 6. *Math1*-Expressing Cells Contribute Fibers to the Dorsal and Ventral Spinocerebellar Tracts as Assayed by DiI Incorporation

(A and B) The dorsal spinocerebellar tracts (dSCT), the external cuneate nucleus (ECN), inferior olive tracts (IO), and the projection to inferior vestibular nucleus (IVN) of control embryos are shown in (A). These tracts are remarkably reduced in *Math1*$^{\beta\text{-Gal}/\beta\text{-Gal}}$ embryos (B and B, inset; two different panels must be used for comparison because of the imaging angle). The reduction in dSCT is best observed in (B), while the reduction in the ECN is best observed in (B, inset).

(C and D) More olivocerebellar fibers are seen crossing the floor plate in control (C) than in *Math1* null embryos.

(E and F) There are fewer parallel fibers in the cerebellum of *Math1* null embryos (F) than wild-type (E), but the fastigial nuclei (NFas) are similar in both.

(G–I) DiI and *LacZ* staining in heterozygote Math1$^{\beta\text{-Gal}/+}$ P0 embryos. *LacZ*-positive cells (green) are clearly identified in the external cuneate nucleus (ECN) (G). DiI was injected into part of the cerebellum to label cranial nerve VIII nuclei and some, but not all, ECN neurons (H). (I) is a composite image of G and H, showing *lacZ*-positive cells colocalized with DiI-positive cells.

Cerebellum (Cb), external cuneate nuclei (ECN), inferior vestibular nucleus (IVN), dorsal medial vesicular neurons (MdD), ventral medial vesicular neurons (MdV), fastigial nuclei (NFas), parallel fibers (Pfib), ventral spinocerebellar tract (VSCT). Scale bar, 100 μm.

stream reporter gene (Akazawa et al., 1995). This suggests that *Math1* may directly activate their expression.

Another gene, *Barhl1,* was recently shown to be expressed in the D1 domain (Saito et al., 1998; Bulfone et al., 2000). *Barhl1* is a member of the Bar family of homeobox proteins, first isolated in *Drosophila* (Kojima et al., 1991). BarH1 and BarH2 control the formation of the R1 and R6 photoreceptors and external sense organs (Higashijima et al., 1992; Higashijima et al., 1992; Kojima et al., 1991). *Barhl1* is not expressed in *Math1* nulls from E10.5 through E13.5 in the developing spinal cord. Analysis of the 5′ sequence of human *BARHL1* reveals four potential E-boxes, including the CAGGTG sequence (S. Banfi, unpublished observation), previously shown to bind *Math1* (Akazawa et al., 1995).

Like LH2A and LH2B, *Barhl1* is not expressed in the absence of *Math1*. This further supports the notion that D1 interneuron precursors fail to differentiate. It is interesting to note that *Barhl1* is also expressed in other regions where *Math1* is expressed, e.g., the cerebellar granule neurons and pontine nucleus (Bulfone et al., 2000). Whether *Barhl1*, LH2A, or LH2B are directly involved in D1 interneuron precursors differentiation is difficult to determine. *Lh2A* and *Lh2B* knockouts have been generated, but there is no report of a spinal cord phenotype (*Lh2A*$^{-/-}$ embryos die in utero with various CNS defects [Porter et al., 1997], whereas *Lh2B*$^{-/-}$ embryos display gonadal abnormalities [Birk et al., 2000]). Functional analysis of these genes suggests that they play roles in cell determination and differentiation, but loss of their expression in *Math1* nulls could be secondary to the primary loss of D1 interneuron precursors.

D1 Interneuron Precursors Migrate Ventrally to Give Rise to Cells of the Spinocerebellar and Cuneocerebellar Tracts

Due to the stability of β-gal (see Figure 2I), as well as the expression of LH2A, LH2B, and *Barhl1* in D1 cells after they migrate, we were able to trace the migration of *Math1*-expressing cells to the deep dorsal horn of the spinal cord. These cells were absent in *Math1* null embryos. In adult mice, this region of the spinal cord contains the spinocerebellar (caudal) and cuneocerebellar (rostral) tracts, which project to the cerebellum and

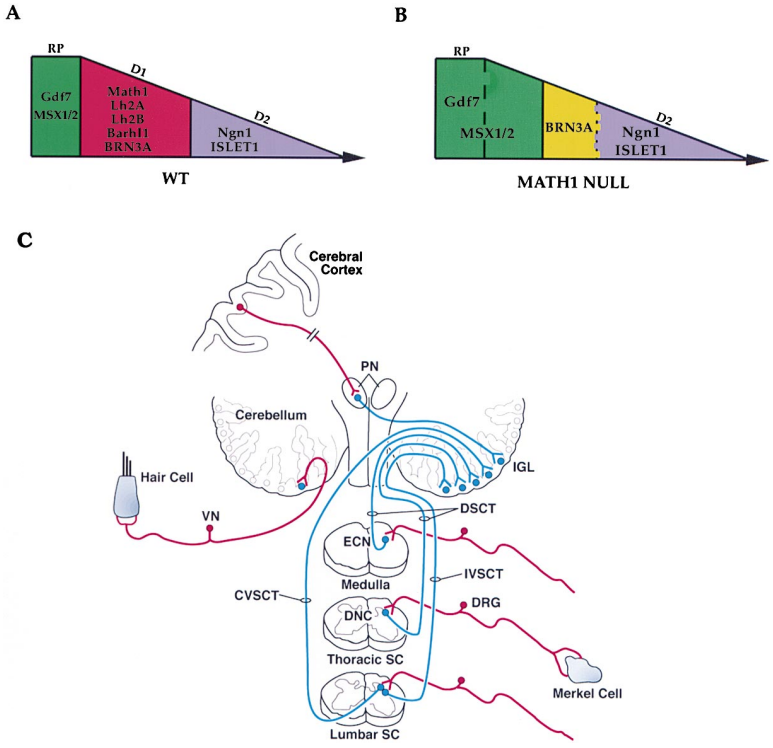

Figure 7. A Model of *Math1* Function in the Development of the Proprioceptive Pathway

(A) In wild-type embryos a BMP gradient is established along the dorsal spinal cord, inducing expression of *Math1*, *Lh2A*, *Lh2B*, *Barhl1*, and BRN3A in the area where the D1 interneurons are being specified.

(B) The BMP gradient is maintained, and the D2 specific markers and *Ngn1* are expressed in the absence of *Math1*. The D1 markers (*Lh2A*, *Lh2B,* and *Barhl1*), however, fail to be expressed, resulting in the loss of neurons whose axons form the SCTs. The MSX1/2 domain expands ventrally, crossing the roof plate/D1 boundary, while BRN3A expression is maintained. Roof plate (RP).

(C) A portion of the proprioceptive pathway (spinothalamic and thalamocortical tracts are not shown); components dependent upon *Math1* are shown in blue.

Pontine nuclei (PN), internal granule layer IGL), dorsal spinocerebellar tract (DSCT), vestibular neuron (VN), external cuneate nucleus (ECN), ipsilateral ventral spinocerebellar tract (IVSCT), contralateral spinocerebellar tract (CVSCT), dorsal nucleus of Clarke (DNC), dorsal root ganglia (DRG), spinal cord (SC).

thalamus. To determine whether these tracts are present in *Math1* nulls, DiI labeling of the tracts was carried out by dye injection into the cerebellum or external cuneate/inferior vestibular nucleus. We found a dramatic decrease in the fiber content of the spino-, olivo-, ponto-, and cuneocerebellar tracts, and the external cuneate nucleus was greatly reduced in size. No differences between wild-type and *Math1* null embryos were observed in the vestibular and reticulocerebellar tracts. The loss of the D1 interneurons and the reduction in the spinocerebellar and cuneocerebellar tracts suggest that the axons of the D1 interneurons form these tracts. This conclusion was further supported by colocalization studies of DiI and *lacZ* activity.

The presence of some fibers in spino-, olivo-, ponto-, and cuneocerebellar tracts suggests that these tracts contain axons whose cell bodies are not dependent on *Math1*. The reduction in the pontocerebellar tracts was not surprising, given the absence of the pontine nuclei in *Math1* null mice as assayed by *lacZ* expression and histopathology (Ben-Arie et al., 2000).

Fate of D1 Precursors in *Math1* Null Mice

If the D1 cell population fails to migrate and form the spinocerebellar and cuneocerebellar tracts, what becomes of D1 precursor cells in *Math1*$^{\beta\text{-Gal}/\beta\text{-Gal}}$ embryos? Staining for apoptotic cells ruled out the possibility that programmed cell death is occurring before E13.5.

Studies of the *Gdf7* knockout mice show that loss of *Math1* expression around E12 results in a dorsal shift of *Ngn1*-positive cells in the developing spinal cord (Lee et al., 1998). This suggests that *Math1* precursor cells might express *Ngn1* in the absence of *Math1*, but our data suggest that *Math1*-expressing cells do not become *Ngn1*-expressing cells in *Math1* nulls. However, we cannot exclude the possibility that some *Ngn1* expression expands into the *Math1* domain. The explanation for our findings may lie in the temporal development of the spinal interneuron precursors and the role of the BMPs in fate specification. Studies by Liem et al. (1997) have shown that dorsally derived explants react in a temporal and spatial fashion when exposed to BMPs; roof plate cells form first, then *Math1*/*Lh2A*/*B*-expressing D1 interneurons, followed by the *Isl1*-expressing D2 class and finally the *lim1/2*-expressing D3 class of interneurons. Therefore, differentiation of different subclasses of spinal interneurons is BMP concentration dependent (Liem et al., 1997). In *Math1* nulls, *Gdf7* is still expressed; the concentration of BMPs may thus remain too high for a fate switch to *Ngn1*-expressing cells. In *Gdf7* nulls, however, the concentration of BMP is reduced, and by E12 the cells respond to the reduced levels of BMPs by expressing *Ngn1* within the *Math1* domain.

Further studies of the dorsal spinal cord revealed an expansion of the MSX1/2 domain. In wild-type embryos MSX1/2 is expressed in the roof plate (Catron et al., 1996; Liem, 1995; Lee et al., 2000) and overlying epidermal ectoderm; its expression is downregulated at the roof plate/D1 boundary (see Figure 5E). Analysis of *Math1* mutants revealed an expansion of the MSX1/2 domain into the D1 domain and colocalization of MSX1/2 with β-Gal. *Msx1* is an immediate early response gene to BMP and is very sensitive to BMP levels. It is thought to play an antineuronal role in development, preventing roof plate cells from undergoing neuronal differentiation (Sasai, 1998). This suggests that in the absence of *Math1*, some of the *Math1*-expressing cells failed to take their proper neuronal fate.

Figure 7 outlines our hypothesis about the fate of the D1 interneurons in the presence and absence of *Math1.* Under normal patterning conditions (Figure 7A), a gradient of BMP signaling is established along the dorsal spinal cord controlling differentiation of the neural crest, roof plate, and D1 and D2 interneurons (Lee et al., 2000; Liem et al., 1997). In this case, the roof plate expresses BMPs (e.g., *Gdf7*) and MSX1/2; the D1 interneuron precursors first express *Math1*, then *Lh2A*, *Lh2B*, *Barhl1,* and *Brn3A*; the D2 interneuron precursors express *Ngn1*, *Isl1*, and probably *Brn3A*. Expression of Math1 is required for the proper expression of *Lh2A*, *Lh2B*, and *Barhl1*, and specification of the D1 interneurons. We therefore favor the hypothesis that *Math1* is involved in the fate determination of the D1 interneurons. In the absence of *Math1,* however, neuronal differentiation in the dorsal spinal cord is altered (Figure 7B). BMPs are expressed normally, inducing formation of the roof plate and D2 interneuron precursors, while the MSX1/2 domain expands laterally crossing the roof plate/D1 boundary. This is consistent with our hypothesis and indicates that some of these cells undergo a fate change (Figure 7B). We propose that BMP concentration and negative regulation by *Math1* define the extent of MSX1/2 expression. Because the BMP gradient is intact, the domain of the D2 neuron precursors does not come to occupy the *Math1* domain.

In conclusion, this study established the essential role of *Math1* in the formation of the proprioceptor pathway. In addition to governing the formation of cerebellar granule cells, pontine neurons, and inner-ear hairs cells, *Math1* plays a key role in the development of the spinocerebellar and cuneocerebellar tracts. In the absence of *Math1,* the D1 neuronal population fails to be specified, resulting in the loss of a subset of fibers forming the spinocerebellar and cuneocerebellar tracts. *Math1* is thus necessary for the autonomous specification of multiple components of a single pathway (Figure 7C). It will be interesting to determine whether the role of *Math1* in specifying multiple components of a sensory pathway is a recurrent theme applicable to other developmentally regulated genes.

Experimental Procedures

Generation of the *Math1* Null Allele

Math1$^{m1/m1}$ knockout mice were generated by replacing the *Math1* open reading frame (ORF) with the selectable marker PGKhprt as previously described by Ben-Arie et al. (1997). *Math1*$^{\beta\text{-Gal}/\beta\text{-Gal}}$ knock-in mice were generated by replacing the *Math1* ORF with a β-galactosidase (β-gal) reporter gene so that β-gal is expressed in all cells that express *Math1* (Ben-Arie et al., 2000).

LacZ Staining and Genotyping of Embryos

Whole-mount *lacZ* staining was carried out on embryos at stages E9.5 to E14.5, as previously described (Ben-Arie et al., 2000). Pregnant females were sacrificed by cervical dislocation; embryos were dissected in ice-cold PBS and fixed for 30 min in 4% paraformaldehyde (PFA) before *lacZ* staining overnight at 30°C (Ben-Arie et al., 1997; Bermingham et al., 1999). After staining, embryos were post-fixed overnight in 4% PFA before embedding in paraplast; 10–45 μm sections were cut using a microtome.

Generation of *Math1*$^{m1/m1:wnt\text{-}1}$

Dr. A. McMahon (Harvard University, Cambridge, MA) kindly provided *Wnt-1-lacZ* transgenic mice expressing β-gal in the neural crest. These mice were timed mated with *Math1*$^{m1/+}$ to generate *Math1*$^{m1/+:wnt\text{-}1}$ mice, which were then backcrossed with *Math1*$^{m1/+}$ mice to generate *Math1*$^{m1/m1:wnt\text{-}1}$ and *Math1*$^{m1/+:wnt\text{-}1}$ embryos. These embryos were collected at E10.5 and genotyped by Southern hybridization (for *Math1* targeting and *lacZ* expression) and PCR (using β-gal specific primers for the presence of the *Wnt-1-lacZ* transgene [Echelard et al., 1994]). Embryos were embedded in paraplast and sectioned as described above.

Immunohistochemistry, Immunofluorescence, and Confocal Microscopy

Immunohistochemistry, immunofluorescence, and confocal microscopy were carried out as previously described (Ben-Arie et al., 1997; Bermingham et al., 1999). Horizontal sections, 12–30 μm, from wild-type, *Math1*$^{\beta\text{-Gal}/+}$, and *Math1*$^{\beta\text{-Gal}/\beta\text{-Gal}}$ null embryos from E10.5 to E13.5 were cut on either a cryostat (immunofluorescence) or microtome (immunohistochemistry). Sections were blocked in 1%–3% normal goat serum and 0.1%–0.3% triton X-100 for 1 hr at room temperature (RT) before incubating overnight at 4°C with primary antibody diluted in blocking solution. Sections were washed three times in PBS at RT before incubating with a secondary antibody conjugated to alkaline phosphatase, Cy3 or Alexa488 fluorphore (diluted in blocking solution) for 2 hr at RT. Sections were washed three times in PBS at RT before being reacted and viewed under a microscope. For double labeling, antibodies were mixed when compatible or were hybridized separately when isolated from the same species. All sections shown were taken from the cervical or thoracic regions of the spinal cord. Anti-2H3 (T. Jessell, Developmental Studies Hybridoma Bank [DSHB]), anti-MSX1/2 (T. Jessell, DSHB), anti-β-galatosidase (Rockland, Gilbersville, PA), anti-BRN3A (E. Turner [Fedtsova and Turner, 1995]), anti-TAG1 (M. Yamamoto, DSHB), anti-DCC (Calbiochem, La Jolla, CA), anti-BrdU (Novacasta, New Castle, UK), anti-LH2A/LH2B (T. Jessell [Lee et al., 1998]), anti-phosphohistone, H3 (Upstate Biotech, Cleveland, OH), and anti-GFAP (Sigma, St. Louis, MO) were used.

RNA In Situ Hybridization

RNA in situ hybridization was carried out as previously described with minor modifications (Albrecht et al., 1997); 12 μm sections were cut from E10.5 to E14.5 embedded embryos. Sections were dried overnight at 30°C before rehydrating, proteinase K treatment, acetylation, and dehydration. S^{35} labeled probes were generated, using the T7/SP6 in vitro transcription kit from Roche-Boehringer Mannheim. Sections were incubated over night at 55°C with 1×10^6 dpm/slide of S^{35} labeled probe. Slides were washed at 62°C in SSC and formamide before RNase A treatment. Sections were dehydrated, dipped in emulsion, developed 2 weeks later, and viewed by indirect microscopy.

Images were captured and color manipulated with Adobe Photoshop. *Barhl1* (Bulfone et al., 2000); *Lh2A, Lh2B*, *Msx1*, and *Gdf7* (T. Jessell [Lee et al., 1998); and *Dcc, Ngn1,* and *Islet1* were generated by subcloning; *trkA* (M. Sanchez) and *trkC* (L. Long) in situ hybridization probes were used.

Apoptosis Studies

Horizontal sections from E10.5 to E13.5 wild-type and *Math1* null embryos were studied using Roche-Boehringer Mannheim in situ cell death detection (TUNEL) kit. Briefly, 12 μm cross sections were cut on a cryostat and air dried 20 min at RT before lysing and reacting as described in the protocol. Sections were counterstained with TOTO-3 iodide (Molecular Probes, Eugene, OR) and viewed under fluorescent microscopy.

DiI Labeling

The lipophilic dicarbocyanine dye, DiI, was injected directly into the cerebellum to label some, but not all, external cuneate/inferior vestibular nucleus of four *Math1*$^{\beta\text{-Gal}/\beta\text{-Gal}}$, four wild-type, and eight *Math1*$^{\beta\text{-Gal}/+}$ E19.5 embryos. DiI was allowed to diffuse for 4 days at 36°C. Injected brains were embedded in gelatin, hardened in 10% PFA and sectioned on a vibratome at 100 μm. Sections were mounted in glycerol and viewed with a compound microscope under rhodamine epifluorescence.

Double labeling with DiI and *lacZ* was carried out in three neonatal

Math1 heterozygote mice according to a previously published protocol (Karis et al., 2001). Mice were cold anesthetized, perfused in 4% PFA, and the brain and spinal cord were freed of the meninges and tested for β-gal activity without detergents. Brains were subsequently transferred into 4% PFA, and DiI was injected into the posterior lobe of the cerebellum. After an appropriate diffusion time, brains and spinal cord were embedded in gelatin and sectioned at 80 μm thickness as described. DiI images were captured by epifluorescence; images of the β-gal reaction product were taken in transmitted light, false colored as green, and combined with the DiI epifluorescence signal. In this way, neither the washing out of DiI (which is absorbed by β-gal blue reaction product) nor the incomplete penetration of the β-gal reaction (in the absence of detergents in the solution) could affect the double labeling that is apparent in all magnifications. The images were superimposed using ImagePro software.

BrdU Incorporation

BrdU labeling was carried out as previously described by Ben-Arie et al. (Ben-Arie et al., 1997). Briefly, at E12.5 a pregnant female was injected with BrdU and sacrificed 2 hr later. Embryos were genotyped and embedded in paraplast. Twelve μm sections from wild-type and *Math1* null embryos were sectioned and treated with hydrochloric acid followed by immunohistochemistry with an anti-BrdU antibody (Novacasta, New Castle, UK).

Acknowledgments

We are grateful to all of the investigators who made reagents available to us: A. McMahon, T. Jessell, E. Turner, M. Sanchez, and L. Long. We also thank D. Armstrong and N. Ben-Arie for advice, B. Antalffy and Richard Atkinson for technical assistance, and D. Trikka and V. Brandt for comments. N.A. Bermingham is an associate fellow; H.Y. Zoghbi and H.J. Bellen are investigators with Howard Hughes Medical Institute. This research was supported in part by the Mental Retardation Research Center, a grant from NIDCD (B.F.), and a postdoctoral fellowship to B.A.H. from the National Institutes of Health.

Received July 6, 2000; revised February 23, 2001.

References

Akazawa, C., Ishibashi, M., Shimizu, C., Nakanishi, S., and Kageyama, R. (1995). A mammalian helix-loop-helix factor structurally related to the product of Drosophila proneural gene atonal is a positive transcriptional regulator expressed in the developing nervous system. J. Biol. Chem. *270*, 8730–8738.

Albrecht, U., Eichele, G., Helms, J., and Lu, H. (1997). Visualization of Gene Expression Patterns by In Situ Hybridization, G.P. Daston, ed. (Boca Raton, FL: CRC Press).

Altman, J., and Bayer, S.A. (1984). The development of the rat spinal cord. Adv. Anat.Embryol. Cell Biol. *85*, 1–166.

Ben-Arie, N., Bellen, H.J., Armstrong, D.L., McCall, A.E., Gordadze, P.R., Guo, Q., Matzuk, M.M., and Zoghbi, H.Y. (1997). Math1 is essential for genesis of cerebellar granule neurons. Nature *390*, 169–172.

Ben-Arie, N., Hassan, B.A., Bermingham, N.A., Malicki, D.M., Armstrong, D., Matzuk, M., Bellen, H.J., and Zoghbi, H.Y. (2000). Functional conservation of atonal and Math1 in the CNS and PNS. Development *127*, 1039–1048.

Bermingham, N.A., Hassan, B.A., Price, S.D., Vollrath, M.A., Ben-Arie, N., Eatock, R.A., Bellen, H.J., Lysakowski, A., and Zoghbi, H.Y. (1999). Math1: an essential gene for the generation of inner ear hair cells. Science *284*, 1837–1841.

Bertuzzi, S., Sheng, H.Z., Copeland, N.G., Gilbert, D.J., Jenkins, N.A., Taira, M., Dawid, I.B., and Westphal, H. (1996). Molecular cloning, structure, and chromosomal localization of the mouse LIM/homeobox gene Lhx5. Genomics *36*, 234–239.

Birk, O.S., Casiano, D.E., Wassif, C.A., Cogliati, T., Zhao, L., Zhao, Y., Grinberg, A., Huang, S., Kreidberg, J.A., Parker, K.L., et al. (2000). The LIM homeobox gene Lhx9 is essential for mouse gonad formation. Nature *403*, 909–913.

Brodal, A. (1981). Neurological Anatomy: In Relation to Clinical Medicine, Third Edition (New York: Oxford University Press).

Brodal, P. (1998). The Central Nervous System: Structure and Function, Second Edition (New York: Oxford University Press).

Bulfone, A., Menguzzato, E., Broccoli, V., Marchitiello, A., Gattuso, C., Mariani, M., Consalez, G.G., Martinez, S., Ballabio, A., and Banfi, S. (2000). Barhl1, a gene belonging to a new subfamily of mammalian homeobox genes, is expressed in migrating neurons of the CNS. Hum. Mol. Genet. *9*, 1443–1452.

Casarosa, S., Fode, C., and Guillemot, F. (1999). Mash1 regulates neurogenesis in the ventral telencephalon. Development *126*, 525–534.

Catron, K.M., Wang, H., Hu, G., Shen, M.M., and Abate-Shen, C. (1996). Comparison of MSX-1 and MSX-2 suggests a molecular basis for functional redundancy. Mech. Dev. *55*, 185–199.

Dodd, J., Morton, S.B., Karagogeos, D., Yamamoto, M., and Jessell, T.M. (1988). Spatial regulation of axonal glycoprotein expression on subsets of embryonic spinal neurons. Neuron *1*, 105–116.

Echelard, Y., Vassileva, G., and McMahon, A.P. (1994). Cis-acting regulatory sequences governing Wnt-1 expression in the developing mouse CNS. Development *120*, 2213–2224.

Fedtsova, N.G., and Turner, E.E. (1995). Brn-3.0 expression identifies early post-mitotic CNS neurons and sensory neural precursors. Mech. Dev. *53*, 291–304.

Fode, C., Gradwohl, G., Morin, X., Dierich, A., LeMeur, M., Goridis, C., and Guillemot, F. (1998). The bHLH protein NEUROGENIN 2 is a determination factor for epibranchial placode-derived sensory neurons. Neuron *20*, 483–494.

Furley, A.J., Morton, S.B., Manalo, D., Karagogeos, D., Dodd, J., and Jessell, T.M. (1990). The axonal glycoprotein TAG-1 is an immunoglobulin superfamily member with neurite outgrowth-promoting activity. Cell *61*, 157–170.

Helms, A.W., and Johnson, J.E. (1998). Progenitors of dorsal commissural interneurons are defined by MATH1 expression. Development *125*, 919–928.

Higashijima, S., Kojima, T., Michiue, T., Ishimaru, S., Emori, Y., and Saigo, K. (1992). Dual Bar homeo box genes of Drosophila required in two photoreceptor cells, R1 and R6, and primary pigment cells for normal eye development. Genes Dev. *6*, 50–60.

Higashijima, S., Michiue, T., Emori, Y., and Saigo, K. (1992). Subtype determination of Drosophila embryonic external sensory organs by redundant homeo box genes BarH1 and BarH2. Genes Dev. *6*, 1005–1018.

Karis, A., Pata, I., van Doornick, J.H., Grosveld, F., de Zeeuw, C.I., de Caprona, D., Fritzsch, B. (2001). Transcription factor GATA-3 alters pathway selection of olivo-cochlear neurons and affects morphogenesis of the ear. J. Comp. Neurol. *429*, 615–630.

Keino-Masu, K., Masu, M., Hinck, L., Leonardo, E.D., Chan, S.S., Culotti, J.G., and Tessier-Lavigne, M. (1996). Deleted in Colorectal Cancer (DCC) encodes a netrin receptor. Cell *87*, 175–185.

Kojima, T., Ishimaru, S., Higashijima, S., Takayama, E., Akimaru, H., Sone, M., Emori, Y., and Saigo, K. (1991). Identification of a different-type homeobox gene, BarH1, possibly causing Bar (B) and Om(1D) mutations in Drosophila. Proc. Natl. Acad. Sci. USA *88*, 4343–4347.

Lee, K.J., Dietrich, P., and Jessell, T.M. (2000). Genetic ablation reveals that the roof plate is essential for dorsal interneuron specification. Nature *403*, 734–740.

Lee, K.J., and Jessell, T.M. (1999). The specification of dorsal cell fates in the vertebrate central nervous system. Annu. Rev. Neurosci. *22*, 261–294.

Lee, K.J., Mendelsohn, M., and Jessell, T.M. (1998). Neuronal patterning by BMPs: a requirement for GDF7 in the generation of a discrete class of commissural interneurons in the mouse spinal cord. Genes Dev.. *12*, 3394–3407.

Liem, K.F., Jr., Tremml, G., and Jessell, T.M. (1997). A role for the roof plate and its resident TGFbeta-related proteins in neuronal patterning in the dorsal spinal cord. Cell *91*, 127–138.

Liem, K.F., Jr., Tremml, G., Roelink, H., and Jessell, T.M. (1995). Dorsal differentiation of neural plate cells induced by BMP-mediated signals from epidermal ectoderm. Cell *82*, 969–979.

Lo, L., Sommer, L., and Anderson, D.J. (1997). MASH1 maintains competence for BMP2-induced neuronal differentiation in post-migratory neural crest cells. Curr. Biol. *7*, 440–450.

Ma, Q., Chen, Z., del Barco Barrantes, I., de la Pompa, J.L., and Anderson, D.J. (1998). neurogenin1 is essential for the determination of neuronal precursors for proximal cranial sensory ganglia. Neuron *20*, 469–482.

Ma, Q., Fode, C., Guillemot, F., and Anderson, D.J. (1999). Neurogenin1 and neurogenin2 control two distinct waves of neurogenesis in developing dorsal root ganglia. Genes Dev. *13*, 1717–1728.

Martin, J.H. (1996). Neuroanatomy: Text and Atlas, Second Edition (Stamford, CT: Appleton and Lange).

Matsumoto, K., Tanaka, T., Furuyama, T., Kashihara, Y., Ishii, N., Tohyama, M., Kitanaka, J., Takemura, M., Mori, T., and Wanaka, A. (1996). Differential expression of LIM-homeodomain genes in the embryonic murine brain. Neurosci. Lett. *211*, 147–150.

Porter, F.D., Drago, J., Xu, Y., Cheema, S.S., Wassif, C., Huang, S.P., Lee, E., Grinberg, A., Massalas, J.S., Bodine, D., et al. (1997). Lhx2, a LIM homeobox gene, is required for eye, forebrain, and definitive erythrocyte development. Development *124*, 2935–2944.

Retaux, S., Rogard, M., Bach, I., Failli, V., and Besson, M.J. (1999). Lhx9: a novel LIM-homeodomain gene expressed in the developing forebrain. J Neurosci *19*, 783–793.

Saito, T., Sawamoto, K., Okano, H., Anderson, D.J., and Mikoshiba, K. (1998). Mammalian BarH homologue is a potential regulator of neural bHLH genes. Dev. Biol. *199*, 216–225.

Sasai, Y. (1998). Identifying the missing links: genes that connect neural induction and primary neurogenesis in vertebrate embryos. Neuron *21*, 455–458.

Tracey, D. (1995). Ascending and descending pathways in the spinal cord. In The Rat Central Nervous System, G. Paxinos, ed. (London: Academic Press), pp. 67–80.

Turner, E.E., Fedtsova, N., and Jeste, D.V. (1997). Cellular and molecular neuropathology of schizophrenia: new directions from developmental neurobiology. Schizophr. Res. *27*, 169–180.

Xu, Y., Baldassare, M., Fisher, P., Rathbun, G., Oltz, E.M., Yancopoulos, G.D., Jessell, T.M., and Alt, F.W. (1993). LH-2: a LIM/homeodomain gene expressed in developing lymphocytes and neural cells. Proc. Natl. Acad. Sci. USA *90*, 227–231.